

Better-Than-Chance Classification for Signal Detection

Jonathan Rosenblatt Roei Gilron Roy Mukamel

August 12, 2016

Abstract

[TODO]

1 Introduction

A common workflow in neuroimaging consists of fitting a classifier, and estimating its predictive accuracy using cross validation. Given that the cross validated accuracy is a random quantity, it is then common to test if the cross validated accuracy is significantly better than chance using a permutation test. Examples in the neuroscientific literature include Golland and Fischl [2003], Pereira et al. [2009], Varoquaux et al. [2016], and especially the recently popularized *multivariate pattern analysis* (MVPA) framework of Kriegeskorte et al. [2006]. This practice is also observed in very high profile publications in the genetics literature: Golub et al. [1999], Slonim et al. [2000], Radmacher et al. [2002], Mukherjee et al. [2003], Juan and Iba [2004], Jiang et al. [2008].

To fix ideas, we will adhere to a concrete example. In Gilron et al. [2016], the authors seek to detect brain regions which encode differences between vocal and non-vocal stimuli. Following the MVPA workflow, the localization problem is cast as a supervised learning problem: if the type of the stimulus can be predicted from the spatial activation pattern significantly better than chance, then a region is declared to encode vocal/non-vocal information. We call this an *accuracy test*, a.k.a. *class prediction*, or *pattern discrimination*.

This same signal detection task can be also approached as a two-group multivariate test. Inferring that a region encodes vocal/non-vocal information, is essentially inferring that the spatial distribution of brain activations is different given a vocal/non-vocal stimulus. As put in Pereira et al. [2009]:

26 ... the problem of deciding whether the classifier learned to dis-
 27 criminate the classes can be subsumed into the more general ques-
 28 tion as to whether there is evidence that the underlying distribu-
 29 tions of each class are equal or not.

30 A practitioner may then call upon a two-group population test such as
 31 Hotelling’s T^2 [Anderson, 2003]. Alternatively, if the size of a brain re-
 32 gion is large compared to the number of observations, so that the spatial
 33 covariance cannot be fully estimated, then a high dimensional version of
 34 Hotelling’s test can be called upon, such as in Schäfer and Strimmer [2005]
 35 or Srivastava [2007]. For brevity, and in contrast to *accuracy tests*, we will
 36 call any two-sample multivariate tests simply *population tests*, also termed
 37 *class comparisons*. [TODO: rename to parameter test?]

38 At this point, it becomes unclear which is preferable: a population test or
 39 an accuracy test? The former with a heritage dating back to Hotelling [1931],
 40 and the latter being extremely popular, as the 959 citations¹ of Kriegeskorte
 41 et al. [2006] suggest.

42 The comparison between location and accuracy tests was precisely the
 43 goal of Ramdas et al. [2016], who compared the T^2 population test to the
 44 accuracy of *Fisher’s linear discriminant analysis* classifier (LDA). By com-
 45 paring the rates of convergence of the powers to 1, Ramdas et al. [2016]
 46 concluded that accuracy and population tests are rate equivalent.

47 Asymptotic relative efficiency measures (ARE) are typically used by statis-
 48 ticians to compare between rate-equivalent test statistics [van der Vaart,
 49 1998]. Ramdas et al. [2016] derive the asymptotic power functions of the
 50 two test statistics, which allows to compute the ARE between Hotelling’s T^2
 51 (location) test and Fisher’s LDA (accuracy) test. Theorem 14.7 of van der
 52 Vaart [1998] relates asymptotic power functions to ARE. Using the results of
 53 Ramdas et al. [2016] we deduce that the ARE is lower bounded by $2\pi \approx 6.3$.
 54 This means that Fisher’s LDA requires at least 6.3 more samples to achieve
 55 the same (asymptotic) power than the T^2 test. In this light, the accuracy
 56 test is remarkably inefficient compared to the population test. For compar-
 57 ison, the t-test is only 1.04 more (asymptotically) efficient than Wilcoxon’s
 58 rank-sum test [Lehmann, 2009], so that an ARE of 6.3 is strong evidence in
 59 favor of the population test.

60 Before discarding accuracy tests as inefficient, we recall that Ramdas
 61 et al. [2016] analyzed a *half-sample* holdout. The authors conjectured that a
 62 leave-one-out approach, which makes more efficient use of the data, may have
 63 better performance. Also, the analysis in Ramdas et al. [2016] is asymptotic.
 64 This eschews the discrete nature of the accuracy statistic, which will be

¹GoogleScholar. Accessed on Aug 4, 2016.

65 shown to have crucial impact. Since typical sample sizes in neuroscience are
 66 not large, we seek to study which test is to be preferred in finite samples?
 67 Our conclusion will be quite simple: *population tests almost always have more*
 68 *power than accuracy tests.*

69 Our statement rests upon the observation that with typical sample sizes,
 70 the accuracy test statistic is highly discrete. Permutation testing with dis-
 71 crete test statistics are known to be conservative [Hemerik and Goeman,
 72 2014], since they are insensitive to mild perturbations of the data, and they
 73 cannot exhaust the permissible false positive rate. The degree of discretiza-
 74 tion is governed by the number of samples. In our neuroscience example
 75 from Gilron et al. [2016], the classification is performed based on 40 trials,
 76 so that the test statistic may assume only 40 possible values. This number
 77 of examples is not unusual if considering this is the number of trial-repeats,
 78 or the number of subjects in an neuroimaging study.

79 The discretization effect is aggravated if the test statistic is highly concen-
 80 trated. For an intuition consider the usage of a the *resubstitution accuracy*
 81 as a test statistic. This statistic simply means that the accuracy is not cross
 82 validated. If the data is high dimensional, the resubstitution accuracy will be
 83 very high due to over fitting. In a very high dimensional model, the resubsti-
 84 tution accuracy will be 1 for the observed data [McLachlan, 1976, Theorem
 85 1], but also for any permutation. The concentration of resubstitution accu-
 86 racy near 1, and its discreteness, render this test completely useless, with a
 87 power tending to 0 for any (fixed) effect size, as the dimension of the model
 88 grows.

89 To compare the power of accuracy tests and population tests in finite sam-
 90 ples, we perform a simulation study of a battery of test statistics. We start
 91 with formalizing the problem in Section 2. The main findings are reported in
 92 Sections 4 and 5. A discussion follows in Section 6.

93 2 Problem setup

94 Let $y \in \mathcal{Y}$ be a class encoding. Let $x \in \mathcal{X}$ be a p dimensional feature vector.
 95 In our vocal/non-vocal example we have $\mathcal{Y} = \{-1, 1\}$ and p , the number of
 96 voxels in a brain region so that $\mathcal{X} = \mathbb{R}^{27}$.

97 Given n pairs of (x_i, y_i) , typically assumed i.i.d., a population test amounts
 98 to testing whether $x|y = 1$ has the the same distribution as $x|y = -1$. I.e.,
 99 we test if the multivariate voxel activation pattern has the same distribution
 100 when given a vocal stimulus, as when given a non-vocal stimulus.

An accuracy test amounts to learning a predictive model $\hat{f}(x)$ from some
 assumed model class $\hat{f} \in \mathcal{F}$. The prediction accuracy, denoted $\mathcal{E}_{\hat{f}}$, is de-

defined as the probability of a given classifier \hat{f} of making a correct prediction. Denoting by $I(A)$ the indicator function of the event A , we get

$$\mathcal{E}_{\hat{f}} := \mathbf{E} \left[I(\hat{f}(x) = y) \right] \quad (1)$$

when given a randomly drawn data point, (x, y) . A statistically significant “better than chance” estimate of $\mathcal{E}_{\hat{f}}$ is evidence that the classes are distinct.

2.1 Candidate Tests

The design of a permutation test using the prediction accuracy, requires the following design choices:

1. Is the statistic cross validated or not?
2. For a V-fold cross validated test statistic:
 - (a) Should the data be refolded in each permutation?
 - (b) Should the data folding be balanced (a.k.a. stratified)?
 - (c) How many folds?
3. How to estimate accuracy?

We will now address these questions while bearing in mind that unlike the typical supervised learning setup, we are not interested in an unbiased estimate of the prediction error, but rather in the mere detection of a difference between two groups.

Cross validate or not? Since we are merely interested in detecting a difference between classes, a biased error estimate is not an issue provided that bias is consistent over all permutations. The underlying intuition is that if the exact same computation is performed over all permutations, then a permutation test will be “fair”, i.e., will not inflate the false positive rate. We will thus be considering both cross validated accuracies, and resubstitution accuracies as our test statistics.

Balanced folding? The standard practice when cross validating is to constrain the data folds to be balanced (i.e. stratified) [e.g. Ojala and Garriga, 2010]. This means that each fold has the same number of examples from each class. We will report results with both balanced and unbalanced data foldings, only to discover, it does not really matter.

128 **Refolding?** The standard practice in neuroimaging is to refold the data
 129 after each permutation, so that data folds are balanced after each label per-
 130 mutation. We will adhere, even though it can be circumvented by permuting
 131 features instead of labels, as done by Golland et al. [2005].

132 **How many folds?** Different authors suggest different rules for the number
 133 of folds. We will be varying the number of folds, and ultimately discover that
 134 the power *decreases with the number of folds*.

How to estimate accuracy? Given a predictor \hat{f} , a natural accuracy test
 statistic is its accuracy $\mathcal{E}_{\hat{f}}$. Since low accuracies, even 0, are evidence that the
 classes are separated, can consider the departure from chance level, $|\mathcal{E}_{\hat{f}} - 0.5|$,
 as the test statistic. For unbalanced classes, chance level is not 0.5, but rather
 the probability of the majority class, we denote by \hat{p}_{max} . This suggests
 the following test statistic $|\mathcal{E}_{\hat{f}} - \hat{p}_{max}|$. Since we will be aggregating these
 statistics over random data sets where \hat{p}_{max} may vary, it seems appropriate to
 standardize the scale of this statistic. We thus propose the z-scored accuracy
 statistic:

$$|\mathcal{E}_{\hat{f}} - \hat{p}_{max}| / \sqrt{\hat{p}_{max}(1 - \hat{p}_{max})}. \quad (2)$$

135 The of tests we will be comparing is collected for convenience in Table 1.

Name	Basis	CV	Accuracy	Parameters
Hotelling	Hotelling	–	–	–
Hotelling.shrink	Hotelling	–	–	–
lda.CV.1	LDA	TRUE	accuracy	–
lda.CV.2	LDA	TRUE	z-accuracy	–
lda.noCV.1	LDA	FALSE	accuracy	–
lda.noCV.2	LDA	FALSE	z-accuracy	–
sd	SD	–	–	–
svm.CV.1	SVM	TRUE	accuracy	cost=1e1
svm.CV.2	SVM	TRUE	accuracy	cost=1e-1
svm.CV.3	SVM	TRUE	z-accuracy	cost=1e1
svm.CV.4	SVM	TRUE	z-accuracy	cost=1e-1
svm.noCV.1	SVM	FALSE	accuracy	cost=1e1
svm.noCV.2	SVM	FALSE	accuracy	cost=1e-1
svm.noCV.3	SVM	FALSE	z-accuracy	cost=1e1
svm.noCV.4	SVM	FALSE	z-accuracy	cost=1e-1

Table 1: This table collects the various test statistics we will be studying. Three are population tests: Hotelling, Hotelling.shrink, and sd. *Hotelling* is the classical two-group T^2 statistic. *Hotelling.shrink* is a high dimensional version with the regularized covariance in Schäfer and Strimmer [2005]. *sd* is another high dimensional version of the T^2 , from Srivastava et al. [2013]. The rest of the tests are variations of the linear SVM, and Fisher’s LDA, with varying accuracy measures, cross validated or not, and varying tuning parameters. For example, *svm.CV.4* is a linear SVM implemented with the *svm* R function, the cost parameter set at 0.1, and using the cross validated z-scored accuracy in Eq. 2. Another example is *lda.noCV.1*, which is Fisher’s LDA, returning the resubstitution accuracy.

136

137 3 Controlling the False Positive Rate

138 Figure 1 demonstrates that all of the tests considered conserve the desired
139 0.05 false positive rate, up to varying levels of conservatism. This can be
140 seen from the fact that the probability of rejection is no larger than 0.05 in
141 the absence of any effect, encoded by a red circle. This is true, in particular
142 if: (a) the folds are balanced or not, (b) the tuning parameters of some test
143 statistic are varied, (d) the number of folds is varied. We also observe that
144 the most conservative tests are the resubstitution accuracy statistics. We
145 return to this matter in the Discussion.

Figure 1: The power of a permutation test with various test statistics. The power on the x axis. Effect are color and shape coded. The various statistics on the y axis. Their details are given in Table 1. Effects vary over 0 (red circle), 0.25 (green triangle), and 0.5 (blue square). Simulation details in Appendix B. Cross-validation was performed with balanced and unbalanced data folding. See sub-captions.



(a) Unbalanced.

(b) Balanced.

4 Power

Having established that all of the tests in our battery control the false positive rate, it remains to be seen if they have similar power—especially when comparing population tests to accuracy tests. From the simulation results reported in Appendix C we collect the following insights:

1. population tests have more power than accuracy tests in all our configurations.
2. The conservativeness decays as the sample grows (Figures 9a, 9b and 10a)
3. For heavy tailed distributions (Figure 8b), the extra power of the location test vanishes.
4. The presence of correlations between coordinates reduces the signal to noise ratio (SNR), thus reduces power. More importantly, in the presence of correlations the effect of regularization is amplified, increasing the power difference between regularized and non-regularized test statis-

161 tics. Put differently- in low SNR regimes, regularization proves crucial
162 (Figure 10b).

163 5. The z-scoring of the accuracies was introduced to deal with unbalanced
164 foldings. If the z-scoring has any effect at all, it merely kills power.

165 6. Both accuracy and population tests are inappropriate for scale alter-
166 natives (Figure 8a). This was to be expected and is reported mostly as
167 a sanity check.

168 7. Balanced folding only affects the z-scored accuracy, in the opposite
169 direction than we anticipated.

170 8. Increasing the SVM’s cost parameter, which reduces the number of
171 support vectors entering the classifier, reduces power.

172 The major insight from simulations is that the use of accuracy tests for
173 signal detection is underpowered compared to population tests. We now
174 verify this finding on a neuroimaging dataset.

175 5 Neuroimaging Example

176 Figure 2 is an application of both a location and an accuracy test to the data
177 of Pernet et al. [2015]. The authors of Pernet et al. [2015] collected fMRI
178 data while subjects were exposed to the sounds of human speech (vocal),
179 and other non-vocal sounds. Each subject was exposed to 20 sounds of each
180 type, totaling in $n = 40$ trials in each scan. The study was rather large and
181 consisted of about 200 subjects. The data was kindly made available by the
182 authors at the OpenfMRI website².

183 We perform group inference using within-subject permutations along the
184 analysis pipeline of Stelzer et al. [2013], which was also reported in Gilron
185 et al. [2016]. For completeness, the pipeline is described in Appendix A. To
186 demonstrate our point, we compare the *sd* population test with the *svm.cv.1*
187 accuracy test.

188 In agreement with our simulation results, the population test (*sd*) discov-
189 ers more brain regions when compared to an accuracy test (*svm.cv.1*). The
190 former discovers 1,232 regions, while the latter only 441, as depicted in Fig-
191 ure 2. We emphasize that both test statistics were compared with the same
192 permutation scheme, and the same error controls, so that any difference in
193 detections is due to their different power.

²<https://openfmri.org/>

194 Having established that accuracy tests are typically underpowered for sig-
 195 nal detection compared to population tests, we wish to identify the conditions
 196 under which this will occur, and discuss practical implications.



Figure 2: Brain regions encoding information discriminating between vocal and non-vocal stimuli. Map reports the centers of 27-voxel sized spherical regions, as discovered by an accuracy test (*svm.cv.1*), and a population test (*sd*). *svm.cv.1* was computed using 5-fold cross validation, and a cost parameter of 1. Region-wise significance was determined using the permutation scheme of Stelzer et al. [2013], followed by region-wise $FDR \leq 0.05$ control using the Benjamini-Hochberg procedure [Benjamini and Hochberg, 1995]. Number of permutations equals 400. The population test detect 1,232 regions, and the accuracy test 441, 399 of which are common to both. For the details of the analysis see Appendix A and Gilron et al. [2016].

197 6 Discussion

198 We have set out to understand which of the tests is more powerful: the ac-
 199 curacy test or the population test. Using simulations, we have concluded
 200 that the population tests are typically preferable. Their high dimensional
 201 versions, such as Srivastava [2007] and Schäfer and Strimmer [2005], are par-
 202 ticularly well suited for neuroimaging problems such as MVPA. We attribute
 203 this to several phenomena: (a) Discretization introduced in finite samples by
 204 the accuracy test statistic. (b) Inefficient use of the data for the validation
 205 holdout set. (c) Regularization crucial in high dimensional problems.

206 The presence of heavy tails shrinks the power advantage of the population
 207 tests over accuracy tests. Our empirical example suggests that even if the
 208 population test does not necessarily dominate the accuracy test in power,
 209 empirically, it does have an advantage.

210 The degree of discretization is governed by the sample size. For this
 211 reason, an asymptotic analysis such as Ramdas et al. [2016] may uncover the
 212 holdout inefficiency, but will not uncover the discretization effect.

213 The practical advice for the practitioner, is that for the purpose of signal
 214 detection, there is typically a population test that is more powerful than
 215 an accuracy test. There is also a good chance that it would be easier to
 216 implement, and faster to run, since no cross validation will be involved.

217 6.1 Ease of implementation

218 A very important consideration is the ease of implementation. The need for
 219 cross validation of the accuracy test greatly increases its computational com-
 220 plexity. Moreover, anyone who has actually implemented tests with discrete
 221 statistics, will attest they are more prone to programming errors. This is
 222 because their unforgiveness to the type of inequalities used. Indeed, mistak-
 223 enly replacing a weak inequality with a strong inequality in one’s program
 224 may considerably change the results. This is not the case for continuous test
 225 statistics.

226 6.2 Reservations

227 Some reservations to the generality of our findings are in order. Firstly,
 228 not all accuracy tests are concerned with signal detection. Consider brain
 229 decoding for machine interfaces, or clinical diagnosis, where the presence of
 230 a medical condition is predicted from imaging data [e.g. Olivetti et al., 2012,
 231 Wager et al., 2013]. In those examples, the purpose of the test is not to
 232 detect a difference between classes, but to actually test the performance of a
 233 particular classifier.

234 Secondly, it may be argued that accuracy tests permits the separation
 235 between classes in high dimensions, such as in *reproducing kernel Hilbert*
 236 *spaces* (RKHS) by using non-linear predictors. This is a false argument—
 237 accuracy test do not have any more flexibility than population tests. Indeed,
 238 it is possible to test for location in the same dimension the classifier is learned.
 239 Gretton et al. [2012] is an example where the test for location is performed
 240 in the RKHS of the data. It is also possible to test for the equality of two
 241 multivariate distributions [TODO: cite vogelstein]. On the other hand, based
 242 on our reported neuroimaging example, and others, we find that a population

243 test in the original feature space is indeed a simple and powerful approach
244 to signal detection.

245 6.3 A good accuracy test

246 For the cases a population test cannot replace an accuracy test, we collect
247 some conclusions and best practices from our simulations. We give particular
248 emphasis in this section to V-fold cross validation due to its popularity, but
249 note that sampling the test set with replacement is actually preferable, as
250 we discuss in Section 6.4.

251 **Sample size.** The conservativeness of accuracy tests decrease with sample
252 size.

253 **Permute features.** Permuting features is easier than permuting labels.
254 It allows to preserve balanced folds after a permutation without refolding.
255 Although we not we did not find a power difference between balanced and
256 unbalanced foldings.

257 **Use less folds.** For V-fold CV, power decreases as the number of folds
258 increases. This is quite interesting since two phenomena compete as the
259 number of folds increase: (a) the train set is larger so that better accuracies
260 are achievable. (b) The test set is smaller so that the accuracy estimate
261 is more variable. The decrease in power with increase fold number suggests
262 that the latter dominates the former. Put differently: it is easier to detect a
263 small stable departure from chance level, than a large but unstable one.

264 **Resubstitution accuracy in low dimension.** Resubstitution accuracy
265 useful in low dimension. In high dimension, the power loss is considerable
266 compared to a cross validated approach. We attribute this to the compounding
267 of discretization and concentration effects: the difference between the
268 sampling distribution of the resubstitution accuracy is simply indistinguishable
269 under the null and under the alternative. In low dimensional problems, the
270 discretization is less impactful, and the computational burden of
271 cross validation can be avoided by using the resubstitution accuracy. There
272 is a fundamental difference between V-folding and resubstitution. The latter
273 should not be thought of as the limit of the former.

274 **Regularize** Regularizing the accuracy test proves very useful in high di-
 275 mensional problems. Put differently: reducing variance by adding some bias
 276 is very useful to detect better-than-chance classification.

277 **Don't z-score.** There is no gain in z-scoring the accuracy scores. Our
 278 motivating rational was clearly flawed. [TODO: why?]

279 6.4 Smoothing accuracy estimates

280 It may be possible to alleviate the effect of discretization by appropriate
 281 cross-validation. The discreteness of the accuracy statistic is goverend by
 282 the number of examples in the union (over all validation iterations) of test
 283 sets. For V-fold CV, for instance, this number is simply the sample size. This
 284 suggests that the accuracy can be “smoothed” by allowing the test sample to
 285 be drawn with replacement. The *bootstrap* may seem like a good candidate
 286 approach since it samples examples with replacement. It does so, however,
 287 for the train set, and not the test set. An algorithm that samples test sets
 288 with replacement is the *leave-one-out bootstrap estimator* (bLOO) and its
 289 derivation– the *0.632 bootstrap estimator* (b0.632) [Hastie et al., 2003, Sec
 290 7.11].

Definition 1 (bLOO). Denoting by $C^{(i)}$ the index set of bootstrap samples,
 b , where observation i is not in the train set, and by \hat{f}^b the classifier fitted to
 the b 'th bootstrap training sample, then the *leave-one-out bootstrap* estimate
 is defined as:

$$\mathcal{E}_{bLOO} := \frac{1}{n} \sum_{i=1}^n \frac{1}{|C^{(i)}|} \sum_{b \in C^{(i)}} I(\hat{f}^b(x_i) = y_i).$$

Equivalently, denoting by $S^{(b)}$ the indexes of observations, i , that are not in
 the bootstrap train sample b ,

$$\mathcal{E}_{bLOO} = \frac{1}{B} \sum_{b=1}^B \frac{1}{|S^{(b)}|} \sum_{i \in S^{(b)}} I(\hat{f}^b(x_i) = y_i).$$

Definition 2 (b0.632). Denoting by \mathcal{E}_{resub} the resubstitution accuracy esti-
 mate, the b0.632 accuracy estimator, $\mathcal{E}_{0.632}$, is defined as

$$\mathcal{E}_{0.632} := 0.368 \mathcal{E}_{resub} + 0.632 \mathcal{E}_{bLOO}.$$

291 Simulation results reported in Figure 3 with naming conventions in Ta-
 292 ble 2. It can be seen that selecting test sets with replacement does increase

the power, when compared to V-fold cross validation, but still falls short from the power of population tests. It can also be seen that power increases with the number of bootstrap replications, itself reducing the level of discretization. The type of bootstrap, bLOO versus b0.632, does not change the power.

Name	Basis	Type	B	Accuracy	Parameters
lda.Boot.1	LDA	b0.632	10	accuracy	—
lda.Boot.2	LDA	bLOO	10	accuracy	—
svm.Boot.1	SVM	b0.632	10	accuracy	cost=1e1
svm.Boot.2	SVM	bLOO	10	accuracy	cost=1e1
svm.Boot.3	SVM	b0.632	50	accuracy	cost=1e1
svm.Boot.4	SVM	bLOO	50	accuracy	cost=1e1

Table 2: The same as Table 1 for bootstrapped accuracy estimates. B-LOO and B-0.632 are defined in definitions 1 and 2 respectively. B denotes the number of Bootstrap samples.

298

299 6.5 High dimensional classifiers

It is known that when $p > n$ Hotelling’s T^2 , and Fisher’s LDA are not computable. In our simulations, in which $p = 23$ and $n = 40$ is “almost” high dimensional, but still allows to compute both tests. We have simulated two high dimensional versions of Hotelling’s T^2 : *sd* [Srivastava, 2007] and *Hotelling.shrink* [Schäfer and Strimmer, 2005]. The former solves the dimensionality problem by assuming independence over coordinates, and the latter by Tikhonov regularization of the covariance, a-la ridge regression. The corresponding high dimensional accuracy tests would be a *naive Bayes* classifier, and l_2 regularized SVM [Ramdas et al., 2016]. We conjecture that they would not alter our conclusions, since the main force driving the conservatism is discretization, which they do not solve.

310



Figure 3: Bootstrap: The power of a permutation test with various test statistics. The power on the x axis. Effect are color and shape coded. The various statistics on the y axis. Their details are given in tables 1 and 2. Effects vary over 0 (red circle), 0.25 (green triangle), and 0.5 (blue square). Simulation details in Appendix B.

Name	Basis	CV	Accuracy	Parameters
svm.highdim.1	SVM	TRUE	accuracy	cost=1e-1
lda.highdim.1	LDA	TRUE	accuracy	—
lda.highdim.2	LDA	TRUE	accuracy	—
lda.highdim.3	LDA	TRUE	accuracy	—

Table 3: The same as Table 1 for regularized (high dimensional) predictors. *svm.highdim.1* is an l_2 regularized SVM Friedman et al. [2010]. *lda.highdim.1* is the Diagonal Linear Discriminant Analysis of Dudoit et al. [2002]. *lda.highdim.2* is the High-Dimensional Regularized Discriminant Analysis of Ramey et al. [2016]. *lda.highdim.3* is the Shrinkage-based Diagonal Linear Discriminant Analysis of Pang et al. [2009].

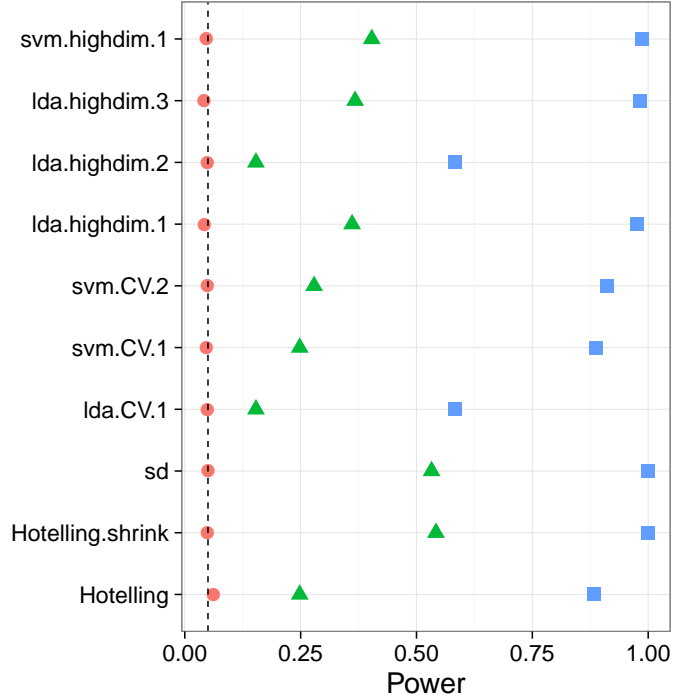


Figure 4: HighDim Classifier: TODO.

6.6 Related Literature

Olivetti et al. [2012] and Olivetti et al. [2014] looked into the problem of choosing a good accuracy test. They propose a new test they call an *independence test*, and demonstrate by simulation that it has more power than other accuracy tests, and can deal with non-balanced data sets. We did not include this test in the battery we compared, but we note the following: (a) The independence test of Olivetti et al. [2012] relies on a discrete test statistic. This means that in the cases that the accuracy test is called upon for discriminating populations, it will probably be underpowered compared to population tests. (b) In contrast with the underlying motivation of Olivetti et al. [2012]’s independence test, we did not find that balancing the data folds is crucial for an accuracy test.

Golland et al. [2005] study accuracy tests using simulation, neuroimaging data, genetic data, and analytically. Their analytic results formalize our intuition from Section 1 on the effect of concentration of the accuracy statistic: The finite Vapnik–Chervonenkis (VC) dimension requirement [Golland and Fischl, 2003, Sec 4.3] prevents the permutation p-value from (asymptotically) concentrating. They also find that the power decreases with the level of dis-

cretization of the statistic. This is seen in their Figure 4, where the size of the test-set, K , governs the discretization. Since they permute features, and not labels, then all their permutation samples are balanced, and there is no issue of refolding.

Golland et al. [2005] simulate the power of an accuracy test using a multivariate Gaussian mixture, with a parameter p governing the separation between classes. Under their model $(x_i|y_i = 1) \sim p\mathcal{N}(\mu_1, I) + (1 - p)\mathcal{N}(\mu_2, I)$ and $(x_i|y_i = -1) \sim (1 - p)\mathcal{N}(\mu_1, I) + p\mathcal{N}(\mu_2, I)$. Varying p interpolates between the null distribution ($p = 0.5$) and a location shift model ($p = 0$). We perform the same simulation as Golland et al. [2005], after reparametrizing p so that $p = 0$ corresponds to the null model, and $p = 23$ to be comparable to our other simulations. We find that in this mixture class of models, like the location class of models, a population test has more power than an accuracy test (Figure 5).

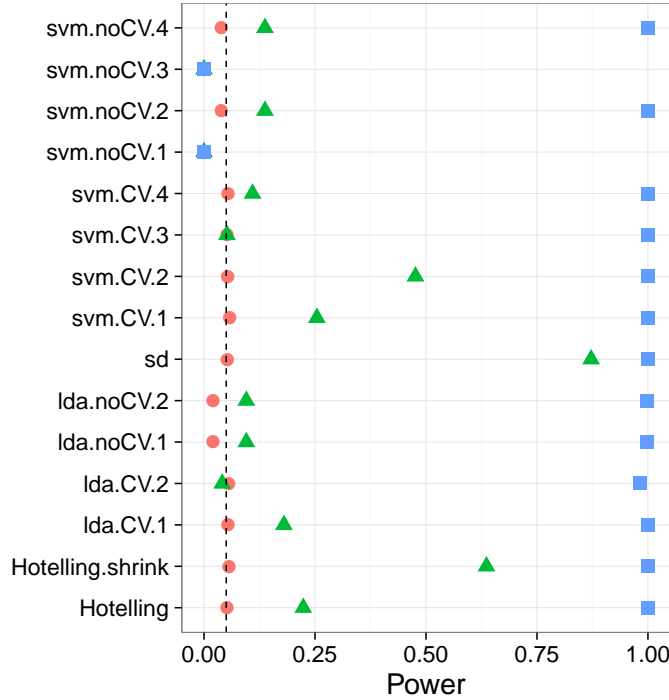


Figure 5: **Mixture:** $\mathbf{x}_i = \chi_i \mu + \eta_i$; $\chi_i = \{-1, 1\}$ and $Prob(\chi_i = 1) = (1/2 - p)^{y_i^*} (1/2 + p)^{1-y_i^*}$. μ is a p -vector with $3/\sqrt{p}$ in all coordinates. The effect, p , is color and shape coded and varies over 0 (red circle), 1/4 (green triangle) and 1/2 (blue square).

344 6.7 Epilogue

345 Given all the above, we find the popularity of accuracy tests quite puzzling.
346 We believe this is due to a reversal of the inference cascade. Researchers first
347 fit a classifier, and then ask if the classes are any different. Were they to
348 start by asking if classes are any different, and only then try to classify, then
349 population tests would naturally arise as the preferred method. As put by
350 Ramdas et al. [2016]:

351 The recent popularity of machine learning has resulted in the ex-
352 tensive teaching and use of prediction in theoretical and applied
353 communities and the relative lack of awareness or popularity of
354 the topic of Neyman-Pearson style hypothesis testing in the com-
355 puter science and related “data science” communities.

356 And more simply by Frank Harrell in the `CrossValidated` Q&A site³:

357 ... your use of proportion classified correctly as your accuracy
358 score. This is a discontinuous improper scoring rule that can be
359 easily manipulated because it is arbitrary and insensitive.

360 7 Acknowledgments

³[http://stats.stackexchange.com/questions/17408/
how-to-assess-statistical-significance-of-the-accuracy-of-a-classifier](http://stats.stackexchange.com/questions/17408/how-to-assess-statistical-significance-of-the-accuracy-of-a-classifier).

References

- T. W. Anderson. *An Introduction to Multivariate Statistical Analysis*. Wiley-Interscience, Hoboken, NJ, 3 edition edition, July 2003. ISBN 978-0-471-36091-9.
- Y. Benjamini and Y. Hochberg. Controlling the false discovery rate: a practical and powerful approach to multiple testing. *JOURNAL-ROYAL STATISTICAL SOCIETY SERIES B*, 57:289–289, 1995.
- S. Dudoit, J. Fridlyand, and T. P. Speed. Comparison of Discrimination Methods for the Classification of Tumors Using Gene Expression Data. *Journal of the American Statistical Association*, 97(457):77–87, Mar. 2002. ISSN 0162-1459. doi: 10.1198/016214502753479248.
- J. Friedman, T. Hastie, and R. Tibshirani. Regularization Paths for Generalized Linear Models via Coordinate Descent. *Journal of Statistical Software*, 33(1):1–22, 2010.
- R. Gilron, J. Rosenblatt, O. Koyejo, R. A. Poldrack, and R. Mukamel. Quantifying spatial pattern similarity in multivariate analysis using functional anisotropy. *arXiv:1605.03482 [q-bio]*, May 2016.
- P. Golland and B. Fischl. Permutation tests for classification: towards statistical significance in image-based studies. In *IPMI*, volume 3, pages 330–341. Springer, 2003.
- P. Golland, F. Liang, S. Mukherjee, and D. Panchenko. Permutation Tests for Classification. In P. Auer and R. Meir, editors, *Learning Theory*, number 3559 in Lecture Notes in Computer Science, pages 501–515. Springer Berlin Heidelberg, June 2005. ISBN 978-3-540-26556-6 978-3-540-31892-7. doi: 10.1007/11503415_34.
- T. R. Golub, D. K. Slonim, P. Tamayo, C. Huard, M. Gaasenbeek, J. P. Mesirov, H. Coller, M. L. Loh, J. R. Downing, M. A. Caligiuri, C. D. Bloomfield, and E. S. Lander. Molecular Classification of Cancer: Class Discovery and Class Prediction by Gene Expression Monitoring. *Science*, 286(5439):531–537, Oct. 1999. ISSN 0036-8075, 1095-9203. doi: 10.1126/science.286.5439.531.
- A. Gretton, K. M. Borgwardt, M. J. Rasch, B. Schölkopf, and A. Smola. A Kernel Two-sample Test. *J. Mach. Learn. Res.*, 13:723–773, Mar. 2012. ISSN 1532-4435.

- 395 T. Hastie, R. Tibshirani, and J. Friedman. *The Elements of Statistical Learning*. Springer, July 2003. ISBN 0-387-95284-5.
- 396
- 397 J. Hemerik and J. Goeman. Exact testing with random permutations. *arXiv:1411.7565 [math, stat]*, Nov. 2014.
- 398
- 399 H. Hotelling. The Generalization of Student’s Ratio. *The Annals of Mathematical Statistics*, 2(3):360–378, Aug. 1931. ISSN 0003-4851, 2168-8990.
- 400
- 401 doi: 10.1214/aoms/1177732979.
- 402 W. Jiang, S. Varma, and R. Simon. Calculating confidence intervals for prediction error in microarray classification using resampling. *Statistical Applications in Genetics and Molecular Biology*, 7(1), 2008.
- 403
- 404
- 405 L. Juan and H. Iba. Prediction of tumor outcome based on gene expression data. *Wuhan University Journal of Natural Sciences*, 9(2):177–182, Mar. 2004. ISSN 1007-1202, 1993-4998. doi: 10.1007/BF02830598.
- 406
- 407
- 408 N. Kriegeskorte, R. Goebel, and P. Bandettini. Information-based functional brain mapping. *Proceedings of the National Academy of Sciences of the United States of America*, 103(10):3863–3868, July 2006. ISSN 0027-8424, 1091-6490. doi: 10.1073/pnas.0600244103.
- 409
- 410
- 411
- 412 E. L. Lehmann. Parametric versus nonparametrics: two alternative methodologies. *Journal of Nonparametric Statistics*, 21(4):397–405, 2009. ISSN 1048-5252. doi: 10.1080/10485250902842727.
- 413
- 414
- 415 G. J. McLachlan. The bias of the apparent error rate in discriminant analysis. *Biometrika*, 63(2):239–244, Jan. 1976. ISSN 0006-3444, 1464-3510. doi: 10.1093/biomet/63.2.239.
- 416
- 417
- 418 S. Mukherjee, P. Tamayo, S. Rogers, R. Rifkin, A. Engle, C. Campbell, T. R. Golub, and J. P. Mesirov. Estimating dataset size requirements for classifying DNA microarray data. *Journal of Computational Biology: A Journal of Computational Molecular Cell Biology*, 10(2):119–142, 2003. ISSN 1066-5277. doi: 10.1089/106652703321825928.
- 419
- 420
- 421
- 422
- 423 M. Ojala and G. C. Garriga. Permutation Tests for Studying Classifier Performance. *Journal of Machine Learning Research*, 11(Jun):1833–1863, 2010. ISSN ISSN 1533-7928.
- 424
- 425
- 426 E. Olivetti, S. Greiner, and P. Avesani. Induction in Neuroscience with Classification: Issues and Solutions. In G. Langs, I. Rish, M. Grosse-Wentrup, and B. Murphy, editors, *Machine Learning and Interpretation*
- 427
- 428

- 429 *in Neuroimaging*, number 7263 in Lecture Notes in Computer Science,
 430 pages 42–50. Springer Berlin Heidelberg, 2012. ISBN 978-3-642-34712-2
 431 978-3-642-34713-9. doi: 10.1007/978-3-642-34713-9_6.
- 432 E. Olivetti, S. Greiner, and P. Avesani. Statistical independence for the
 433 evaluation of classifier-based diagnosis. *Brain Informatics*, 2(1):13–19, Dec.
 434 2014. ISSN 2198-4018, 2198-4026. doi: 10.1007/s40708-014-0007-6.
- 435 H. Pang, T. Tong, and H. Zhao. Shrinkage-based Diagonal Discriminant
 436 Analysis and Its Applications in High-Dimensional Data. *Biometrics*, 65
 437 (4):1021–1029, Dec. 2009. ISSN 1541-0420. doi: 10.1111/j.1541-0420.2009.
 438 01200.x.
- 439 F. Pereira, T. Mitchell, and M. Botvinick. Machine learning classifiers and
 440 fMRI: A tutorial overview. *NeuroImage*, 45(1, Supplement 1):S199–S209,
 441 Mar. 2009. ISSN 1053-8119. doi: 10.1016/j.neuroimage.2008.11.007.
- 442 C. R. Pernet, P. McAleer, M. Latinus, K. J. Gorgolewski, I. Charest, P. E. G.
 443 Bestelmeyer, R. H. Watson, D. Fleming, F. Crabbe, M. Valdes-Sosa, and
 444 P. Belin. The human voice areas: Spatial organization and inter-individual
 445 variability in temporal and extra-temporal cortices. *NeuroImage*, 119:164–
 446 174, Oct. 2015. ISSN 1053-8119. doi: 10.1016/j.neuroimage.2015.06.050.
- 447 M. D. Radmacher, L. M. McShane, and R. Simon. A Paradigm for
 448 Class Prediction Using Gene Expression Profiles. *Journal of Computa-*
 449 *tional Biology*, 9(3):505–511, June 2002. ISSN 1066-5277. doi: 10.1089/
 450 106652702760138592.
- 451 A. Ramdas, A. Singh, and L. Wasserman. Classification Accuracy as a Proxy
 452 for Two Sample Testing. *arXiv:1602.02210 [cs, math, stat]*, Feb. 2016.
- 453 J. A. Ramey, C. K. Stein, P. D. Young, and D. M. Young. High-Dimensional
 454 Regularized Discriminant Analysis. *arXiv preprint arXiv:1602.01182*,
 455 2016.
- 456 J. Schäfer and K. Strimmer. A Shrinkage Approach to Large-Scale Covariance
 457 Matrix Estimation and Implications for Functional Genomics. *Statistical*
 458 *Applications in Genetics and Molecular Biology*, 4(1), Jan. 2005. ISSN
 459 1544-6115. doi: 10.2202/1544-6115.1175.
- 460 D. K. Slonim, P. Tamayo, J. P. Mesirov, T. R. Golub, and E. S. Lander. Class
 461 Prediction and Discovery Using Gene Expression Data. In *Proceedings of*
 462 *the Fourth Annual International Conference on Computational Molecular*

- 463 *Biology*, RECOMB '00, pages 263–272, New York, NY, USA, 2000. ACM.
464 ISBN 978-1-58113-186-4. doi: 10.1145/332306.332564.
- 465 M. S. Srivastava. Multivariate Theory for Analyzing High Dimensional Data.
466 *Journal of the Japan Statistical Society*, 37(1):53–86, 2007. doi: 10.14490/
467 jjss.37.53.
- 468 M. S. Srivastava, S. Katayama, and Y. Kano. A two sample test in high
469 dimensional data. *Journal of Multivariate Analysis*, 114:349–358, Feb.
470 2013. ISSN 0047-259X. doi: 10.1016/j.jmva.2012.08.014.
- 471 J. Stelzer, Y. Chen, and R. Turner. Statistical inference and multiple test-
472 ing correction in classification-based multi-voxel pattern analysis (MVPA):
473 Random permutations and cluster size control. *NeuroImage*, 65:69–82, Jan.
474 2013. ISSN 1053-8119. doi: 10.1016/j.neuroimage.2012.09.063.
- 475 A. W. van der Vaart. *Asymptotic Statistics*. Cambridge University Press,
476 Cambridge, UK ; New York, NY, USA, Oct. 1998. ISBN 978-0-521-49603-
477 2.
- 478 G. Varoquaux, P. R. Raamana, D. Engemann, A. Hoyos-Idrobo, Y. Schwartz,
479 and B. Thirion. Assessing and tuning brain decoders: cross-validation,
480 caveats, and guidelines. working paper or preprint, June 2016.
- 481 T. D. Wager, L. Y. Atlas, M. A. Lindquist, M. Roy, C.-W. Woo, and E. Kross.
482 An fMRI-Based Neurologic Signature of Physical Pain. *New England Jour-
483 nal of Medicine*, 368(15):1388–1397, Apr. 2013. ISSN 0028-4793. doi:
484 10.1056/NEJMoa1204471.

485 A Analysis pipeline

486 Here is the analysis pipeline of Stelzer et al. [2013] we for the auditory data in
 487 Gilron et al. [2016]. Denoting by $i = 1, \dots, I$ the subject index, $v = 1, \dots, V$
 488 the voxel index, and $s = 1, \dots, S$ the permutation index. Since regions⁴ are
 489 centered around a unique voxel, the voxel index v also serves as a unique
 490 region index. Algorithm 1 computes a region-wise test statistic, which is
 491 compared to its permutation null distribution computed by Algorithm 2.

Algorithm 1: Compute a group parametric map.

Data: fMRI scans, and experimental design.
Result: Brain map of group statistics: $\{\bar{T}_v\}_{v=1}^V$

```

1 for  $v \in 1, \dots, V$  do
2   for  $i \in 1, \dots, I$  do
3      $T_{i,v} \leftarrow$  test statistic for subject  $i$  in a region centered at  $v$ .
4    $\bar{T}_v \leftarrow \frac{1}{I} \sum_{i=1}^I T_{i,v}$ .
```

Algorithm 2: Compute a permutation p-value map.

Data: fMRI scans of 20 subjects, experimental design.
Result: Brain map of permutation p-values: $\{p_v\}_{v=1}^V$

```

1 for  $s \in 1, \dots, S$  do
2   permute labels;
3    $\bar{T}_v^s \leftarrow$  parametric map
```

⁴*searchlight* or *sphere* in the MVPA parlance

494 B Simulation Details

495 The following details are common to all the reported simulations, unless stated
496 otherwise in a figure’s caption. The R code for the simulations can be found
497 in [TODO].

498 Each simulation is based on 4,000 replications. In each replication, we
499 generate n i.i.d. samples from a shift model $\mathbf{x}_i = \mu \mathbf{y}_i^* + \eta_i$. Where $y_i^* = \{0, 1\}$
500 is the class of subject i in dummy coding. Recalling that $y_i = \{-1, 1\}$ is the
501 class in effect coding, then clearly $y_i = 2y_i^* - 1$. The noise is distributed as
502 $\eta_i \sim \mathcal{N}_p(0, \Sigma)$. The sample size $n = 40$. The dimension of the data is $p = 23$.
503 The covariance $\Sigma = I$. Effects, i.e. shifts μ , are equal coordinate p -vectors
504 with coordinates that vary over $\mu \in \{0, 1/4, 1/2\}$.

505 Having generated the data, we compute each of the test statistics in Ta-
506 ble 1. For test statistics that require data folding, we used 8 folds. We then
507 compute a permutation p-value by permuting the class labels, and recomput-
508 ing each test statistic. We perform 400 such permutations. We then reject
509 the $\mu_i = 0$ null hypothesis if the permutation p-value is smaller than 0.05.
510 The reported power is the proportion of replication where the permutation
511 p-value falls below 0.05.

C Simulation Results

Figure 6: Simulation details in Appendix B except the changes in the sub-captions.

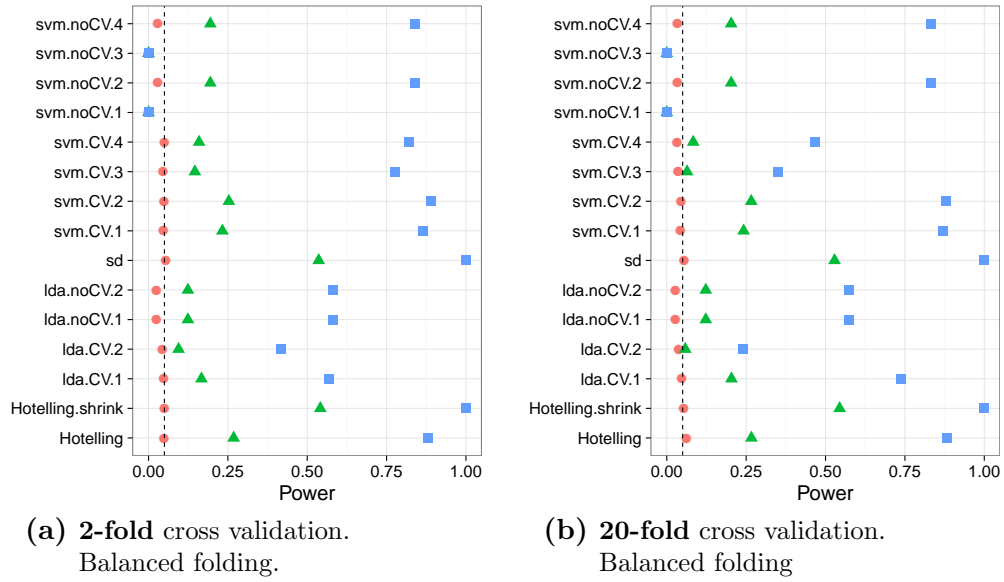


Figure 7: Simulation details in Appendix B except the changes in the sub-captions.



Figure 8: Simulation details in Appendix B except the changes in the sub-captions.

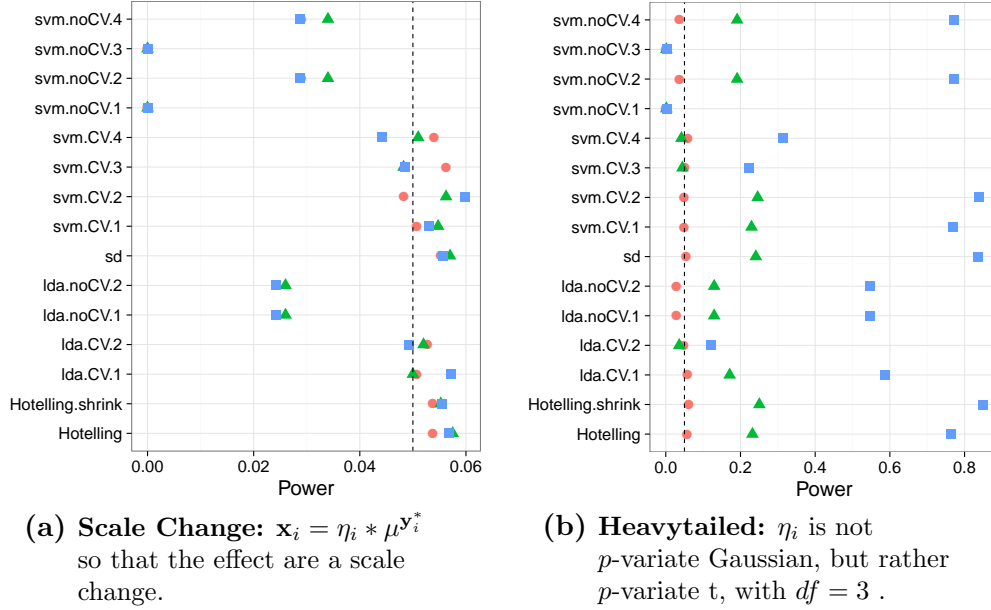
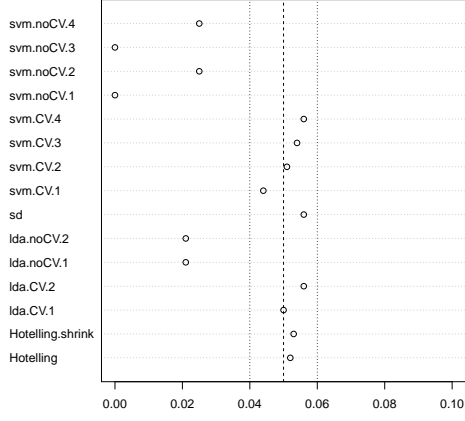
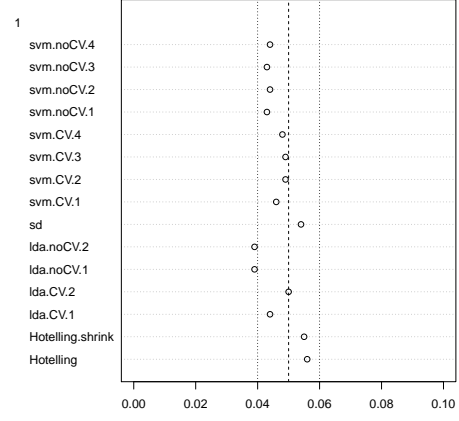


Figure 9: Simulation details in Appendix B except the changes in the sub-captions.

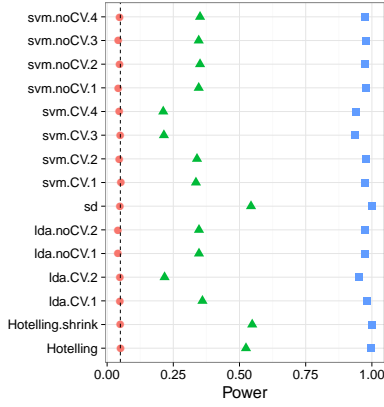


(a) **Low-Dimension:** False positive rates for $n = 40$.

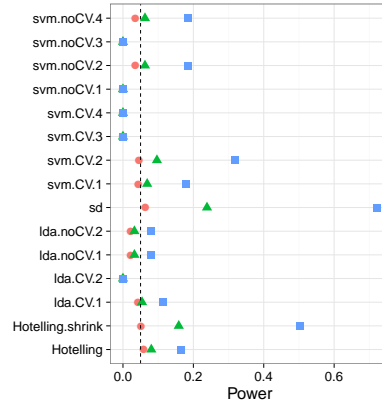


(b) **High-Dimension:** False positive rates for $n = 400$.

Figure 10: Simulation details in Appendix B except the changes in the sub-captions.



(a) **High-Dimension, local alternative:**
 $n = 400$,
 $\mu \in \frac{1}{\sqrt{10}} \times \{0, 1/4, 1/2\}$.



(b) **AR(1) dependence:**
 $\Sigma_{k,l} = \rho^{|k-l|}; \rho = 0.8$.